ECS Journal of Solid State Science and Technology

OPEN ACCESS

Local, Temperature-Dependent Trapping and Detrapping in the $LiGa_5O_8$:Cr Infrared Emitting Persistent Phosphor

To cite this article: Olivier Q. De Clercq and Dirk Poelman 2018 *ECS J. Solid State Sci. Technol.* **7** R3171

View the article online for updates and enhancements.

You may also like

- Optical Dielectric Function Modeling and Electronic Band Lineup Estimation of Amorphous High-k $LaGdO_3$ Films
S. P. Pavunny, R. Thomas, A. Kumar et al.
- Optimization studies on output stabilization time and graphene oxide concentration in graphene-based flexible micro-supercapacitor
Sangeetha Gopan G S, Nelsa Abraham, Harikrishnan R S et al.
- Growth Behavior of m-Plane ZnO Epilayer on (100) $LiGaO_2$ by Chemical Vapor Deposition
Jun-Yi Yu, Teng-Hsing Huang, Liuwen Chang et al.

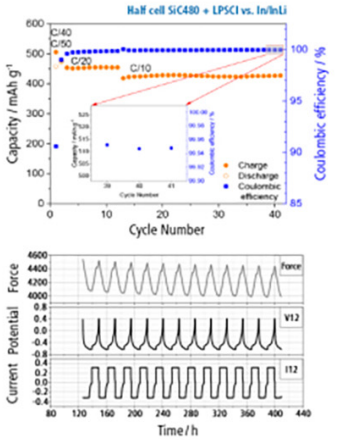
The New PAT-Cell-Solid!

EL-CELL® electrochemical test equipment

Cycle Solid-State Batteries Under Controlled Pressure of up to 300 MPa (6 mm Diameter)!



- Adjust and measure a force of up to 9000 N on the cell stack!
Force adjustment possible throughout the entire experiment
- Built-in force, and temperature sensors!
With optional gas pressure sensor and gas in- and outlet
- PAT-Solid-Core for easy assembly and reproducible results!
Press and cycle solid-state batteries with 6 or 10 mm electrode diameter
- Cableless and highly sealed battery test cell!
For precise long-term measurements of solid-state cell chemistries



Learn more on our product website:

Scan me!

Download the data sheet (PDF):

Scan me!

Or contact us directly:

+49 40 79012-734

sales@el-cell.com

www.el-cell.com

This content was downloaded from IP address 15.204.172.39 on 14/11/2026 at 13:14

JSS Focus Issue on Visible and Infrared Phosphor Research and Applications

Local, Temperature-Dependent Trapping and Detrapping in the $LiGa_5O_8$:Cr Infrared Emitting Persistent Phosphor

Olivier Q. De Clercq [a,b] **and Dirk Poelman** [a,b,*,z]

[a] *LumiLab, Department of Solid State Sciences, Ghent University, Ghent, Belgium*
[b] *Center for Nano- and Biophotonics (NB-Photonics), Ghent University, Ghent, Belgium*

The near-infrared emitting persistent phosphor $LiGa_5O_8:Cr^{3+}$ (LGO:Cr) has promising applications in bioimaging. In order to improve the persistent luminescence of LGO:Cr and other Cr-doped persistent phosphors, a better understanding of trapping and detrapping mechanisms is necessary. In this work, we study the afterglow and thermoluminescence via a thermal fading experiment. The results show that there is a broad trap distribution present in LGO:Cr. The emission spectrum of chromium changes during the afterglow, which indicates that different Cr ions experience a varying crystal field in the LGO host, due to different defect configurations, and that the detrapping process occurs locally. The results of thermoluminescence and spectral decay measurements show that chromium ions residing near deep traps are subject to a smaller crystal field. Vacancies formed during the synthesis are most probably causing this effect. Codoping LGO with Si^{4+} or Ge^{4+} significantly improves the persistent luminescence and increases the number of deep-lying traps in the phosphor.

© The Author(s) 2017. Published by ECS. This is an open access article distributed under the terms of the Creative Commons Attribution 4.0 License (CC BY, http://creativecommons.org/licenses/by/4.0/), which permits unrestricted reuse of the work in any medium, provided the original work is properly cited. [DOI: 10.1149/2.0211801jss] All rights reserved.

Manuscript submitted August 7, 2017; revised manuscript received September 21, 2017. Published October 20, 2017. *This paper is part of the JSS Focus Issue on Visible and Infrared Phosphor Research and Applications.*

In recent years, interest in transition metal-doped persistent phosphors has increased significantly because of their potential for biomedical imaging.[1–4] Chromium-doped gallates especially, have been studied intensively because of their near-infrared emission, situated in the first tissue transparency window (between 650 and 950 nm[5]), and their long afterglow times.[6–9] Research on Cr-doped nanophosphors has shown that these materials have good chemical stability and low toxicity, necessary conditions for imaging applications.[3,10,11]

Persistent luminescence is the phenomenon where a phosphor keeps emitting light for seconds, minutes, or even hours after the excitation has stopped.[12,13] In general, part of the light energy during excitation is stored inside the host material. This charging of persistent phosphors involves charge carriers that are trapped in defect energy states inside the bandgap of the semiconducting or insulating host. The type of trapped charge carrier can differ between persistent phosphors. In the case of $SrAl_2O_4$:Eu,Dy, electrons were determined to be the trapped carriers, and a corresponding valence change of the Eu ions during excitation was found via X-ray absorption measurements.[14] For chromium-based persistent phosphors, no such valence changes could be measured yet, which suggests that both electrons and holes are separated from the Cr^{3+} ion during the charging step.[15,16]

Thus, significant progress has been made in the past 20 years on elucidating the mechanisms behind trapping and detrapping, as well as revealing the defect nature of the traps, in some of the more well-known and commercially viable persistent phosphors.[12,15,17,18]

However, the mechanism behind the persistent luminescence is still unclear for many materials, and depends on the specific phosphor under study. A better understanding of the trap system should lead to a more targeted tuning of the phosphor to increase the trapping capacity of these phosphors and thus improve their utility for imaging applications.

In this work, we focus on the phosphor $LiGa_5O_8:Cr^{3+}$ (LGO:Cr) with emission around 720 nm and outstanding afterglow properties.[8,19,20]

The afterglow profile of LGO:Cr shows an approximate linear t^{-1} behavior, which has been linked to either a tunneling mechanism[20–22] or a thermally activated detrapping process from a broad distribution of traps in the host.[23–25] Via a combination of afterglow and thermoluminescence (TL) measurements, we reveal the presence of a trap distribution in the host. Thermal fading experiments allow us to study the temperature dependence of the detrapping process. Monitoring changes of the Cr^{3+} emission spectrum with time reveals that only a specific subset of Cr ions is taking part in the long persistent luminescence.

TL of LGO:Cr samples codoped with either Si^{4+} or Ge^{4+} shows that the glow curves shift to higher temperatures upon codoping, indicating the increase in the number of deeper-lying trap states. Both M^{4+} ions significantly enhance the afterglow time of the LGO phosphor to over 8 hours, before intensity drops below 10^{-3} mW sr^{-1} m^{-2}.

Experimental

LGO:Cr powder samples were prepared via solid state reaction. Li_2CO_3 (99.998%, Alfa Aesar) and Ga_2O_3 (99.99%, Alfa Aesar) were mixed and ground in an agate mortar. Cr was added as Cr_2O_3 (99.97%, Alfa Aesar) with a molar concentration of 1% with respect to the Ga content. GeO_2 (99.999%, Alfa Aesar) or SiO_2 (99.9%, Alfa Aesar), respectively, was added to the LGO spinel structure according to the substitution $LiGa_{5-x}M_xO_8:Cr^{3+}$ (M = Si or Ge; x = 0.4).

This starting mixture was transferred to open alumina crucibles and heated in ambient air, first to 800°C for 2 h in order to remove the carbon content in the precursors, and subsequently to 1300°C for 4 h to form the final host. The employed heating rate was 300°C h^{-1}. After synthesis, the samples were allowed to cool naturally overnight.

Photoluminescence (PL) emission and decay of the samples were measured using a fluorescence spectrometer (FS920, Edinburgh Instruments) using a monochromated 450 W Xe-arc as the excitation source. All spectra were automatically corrected for detector response.

Afterglow decay profiles were measured with a Centronic OSD100-5T silicon photodiode, calibrated in absolute radiometric units and connected to a Hamamatsu C9329 photosensor amplifier. Prior to afterglow measurements, the samples were excited for 5 min by 1000 lx light of an unfiltered Xenon arc lamp.

TL was recorded in a homebuilt setup, details of which can be found in Botterman et al.[26] Before each TL measurement, the sample was thermally cleaned by heating to 220°C, thereby emptying the trapping states. The samples were optically charged using the 254 nm emission line of a 3 W Hg-lamp during 10 min at 20°C. After charging, the sample was kept at 20°C for 10 min before heating and recording of the TL output. During the heating step, a constant heating rate, β, of 15°C min^{-1} was used.

*Electrochemical Society Member.
[z]E-mail: Dirk.Poelman@UGent.be

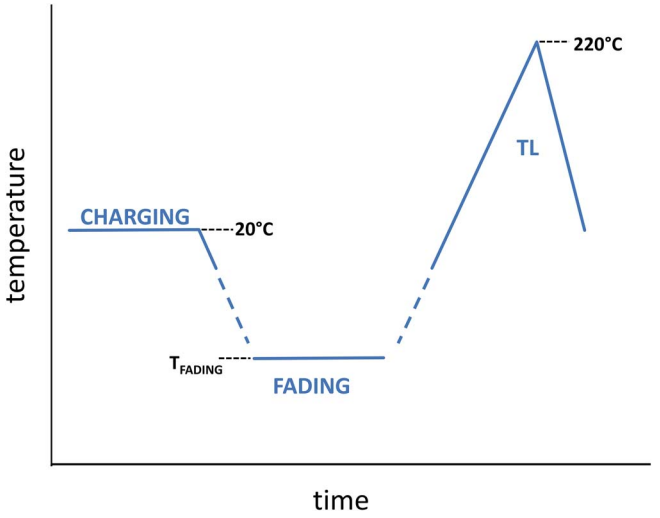


Figure 1. Experimental procedure for the thermal fading experiment. Charging of the sample at 20°C for 10 min with 254 nm excitation light, is followed by a rapid cooling to a specific fading temperature, T_{FADING}. The sample is held there for a fixed amount of time (1 min, 10 min or 30 min), after which it is heated to 220°C for the TL recording. The heating rate during the TL recording is linear and fixed at 15 K min^{-1}.

The light emitted from the phosphor during charging, afterglow, and TL was collected and guided by an optical fiber to a ProEM1600 EMCCD camera attached to an Acton SP2300 monochromator (Princeton Instruments).

To investigate the temperature dependence of the detrapping, a thermal fading experiment was conducted in the following way (see Figure 1 for a schematic outline):

The sample was charged for 10 min at 20°C. After charging, the sample was cooled ($\beta = 30$ K min^{-1}) using a liquid nitrogen flow to a specific temperature, T_{FADING}, where it was kept for either 1 min, 10 min or 30 min. After this fading time, the sample was heated to 220°C ($\beta = 15$°C min^{-1}) while recording the light output every K. T_{FADING} was −60°C, −40°C, −20°C, −10°C, 0°C or 10°C.

Results and Discussion

Figure 2 shows the afterglow profiles of the LGO:M,Cr samples at room temperature. The afterglow time – defined as the time it takes for the intensity to drop below 10^{-3} mW sr^{-1} m^{-2} – for LGO:Cr is about 2 hours for a powder sample. This afterglow time can be significantly improved to over 8 hours by codoping with ions with a 4+ valence, such as Si or Ge.[19]

Plotting the inverse of the afterglow intensity against time reveals an approximately linear t^{-1} behavior for the persistent luminescence (Figure 2). This specific decay behavior has been linked to either a detrapping mechanism from isolated traps via tunneling processes;[21] or an indication for the presence of a broad trap distribution in the phosphor.[23,24,27,28] In general, one can distinguish between the two processes by checking the temperature dependence of the afterglow and thermoluminescence behavior.[27]

Figure 3 shows a recorded TL curve for LGO:Cr after charging at 20°C for 10 min. A broad intensity profile was measured with a maximum around 60°C, a shoulder around 100°C and a broad, continuous TL signal above 150°C. The TL profile is comparable in shape with the previously obtained profiles for LGO, but with maxima shifted to lower temperatures due to a smaller heating rate (15°C min^{-1} instead of 4°C s^{-1}).[8] The broad glow curve with shoulder and a continuum signal at high temperatures already strongly indicates the presence of multiple trap levels in the material. The continuum signal is an aggregate TL signal from multiple, close-lying, deeper trapping states.[25] The relatively large noise level of the measurement is

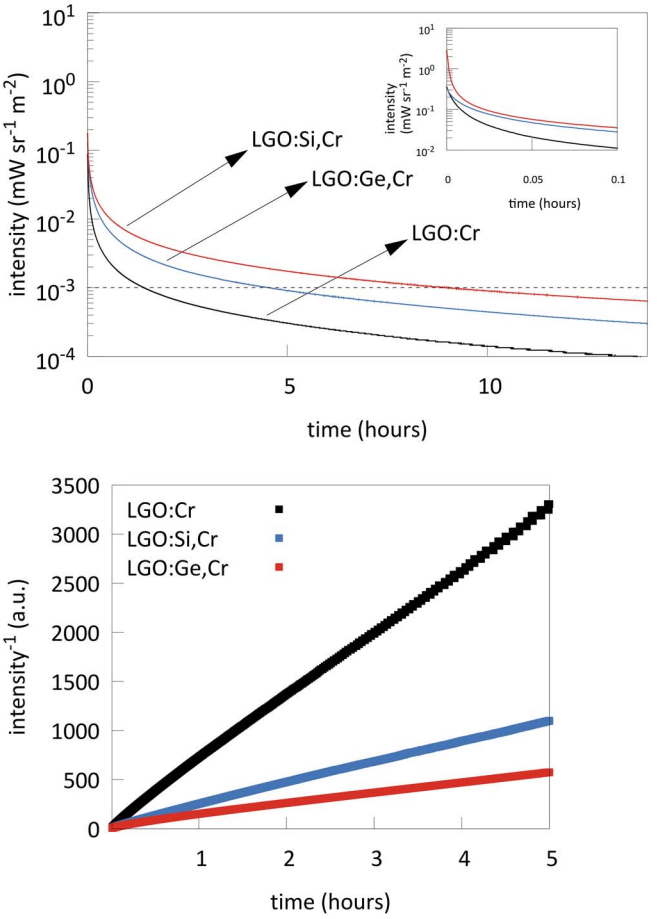


Figure 2. (top) Afterglow decay curves for LGO:Cr (black), LGO:Si,Cr (red) and LGO:Ge,Cr (blue). The afterglow time is defined as the time when the intensity decreases below 10^{-3} mW sr^{-1} m^{-2} (dashed line). Inset: afterglow intensity of the measured samples for 0.1 h after excitation. (bottom) Linear t^{-1} behavior for the LGO:M,Cr phosphors indicates either a tunneling mechanism or the presence of a trap distribution.

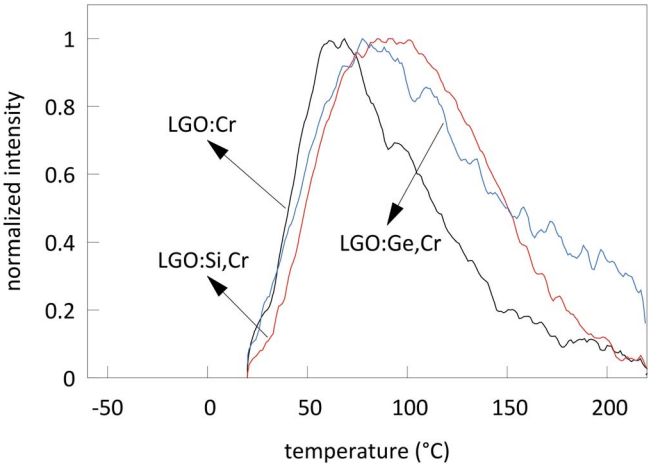


Figure 3. Normalized thermoluminescence glow curve for LGO:M,Cr, after charging at 20°C for 10 min with 254 nm excitation light. Recording of the TL started 10 min after the stopping of the excitation. By codoping with Si^{4+} or Ge^{4+}, the TL signal shifts to higher temperatures, indicating an increase in the number of deep traps.

indicative of the limited light output corresponding to the low heating rate and the low sensitivity of the EMCCD detector in this wavelength range.

As a side note, all TL curves presented in this work were not corrected for thermal quenching as the relative PL intensity hardly decreases from 100% at 20°C to ∼93% at 220°C (Figure 4). This limited quenching is also observed in other Cr-doped systems,[29] and is caused by an increase of broad-band emission from the Cr $^4T_2$ state with increasing temperature (see Figure 6 for the emission profile of LGO). In this way, the strong quenching of the narrow-band emission from the Cr ^2E state is compensated.

The previously proposed mechanism for the persistent luminescence in LGO:Cr is tunneling from deep-lying traps to the Cr activator. Liu and coworkers concluded this by measuring afterglow at liquid nitrogen temperature (LNT) and subsequently recording the TL output.[8] They showed that shallow traps exist in LGO for which TL intensity is recorded below room temperature (RT). These shallow traps are not filled when LGO is charged at RT and subsequently cooled down to LNT. The fact that afterglow could still be recorded at LNT, but no TL signal at low temperatures was measured, is an indication that tunneling can occur from deeper lying trap states to the Cr ion at low temperatures.

However, our fading measurements, as outlined in Figure 1, also show a clear temperature dependence for the detrapping from deeper traps (Figure 5). The shape and intensity of the TL peak at 60°C

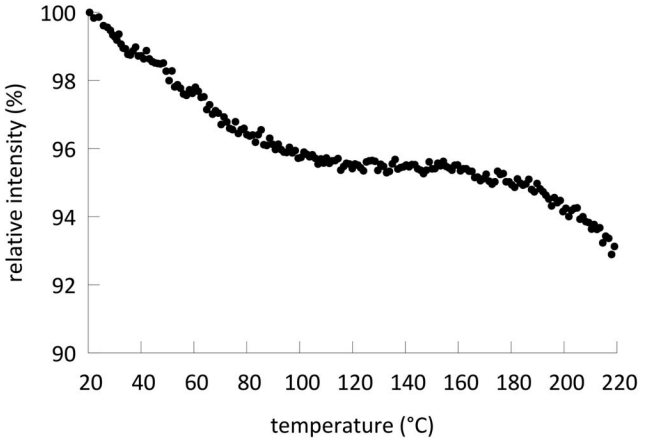


Figure 4. Thermal quenching behavior for LGO:Cr up to 220°C. The total intensity at each temperature point was obtained by integrating the emission spectrum of Cr^{3+} between 650 nm and 800 nm.

remains constant for the fading experiments at temperatures below −20°C (Figures 5a–5e), and no decrease of the TL signal is observed.

From −10°C, a shift in the TL curve becomes pronounced at the low-temperature side of the TL peak for increasing fading times and

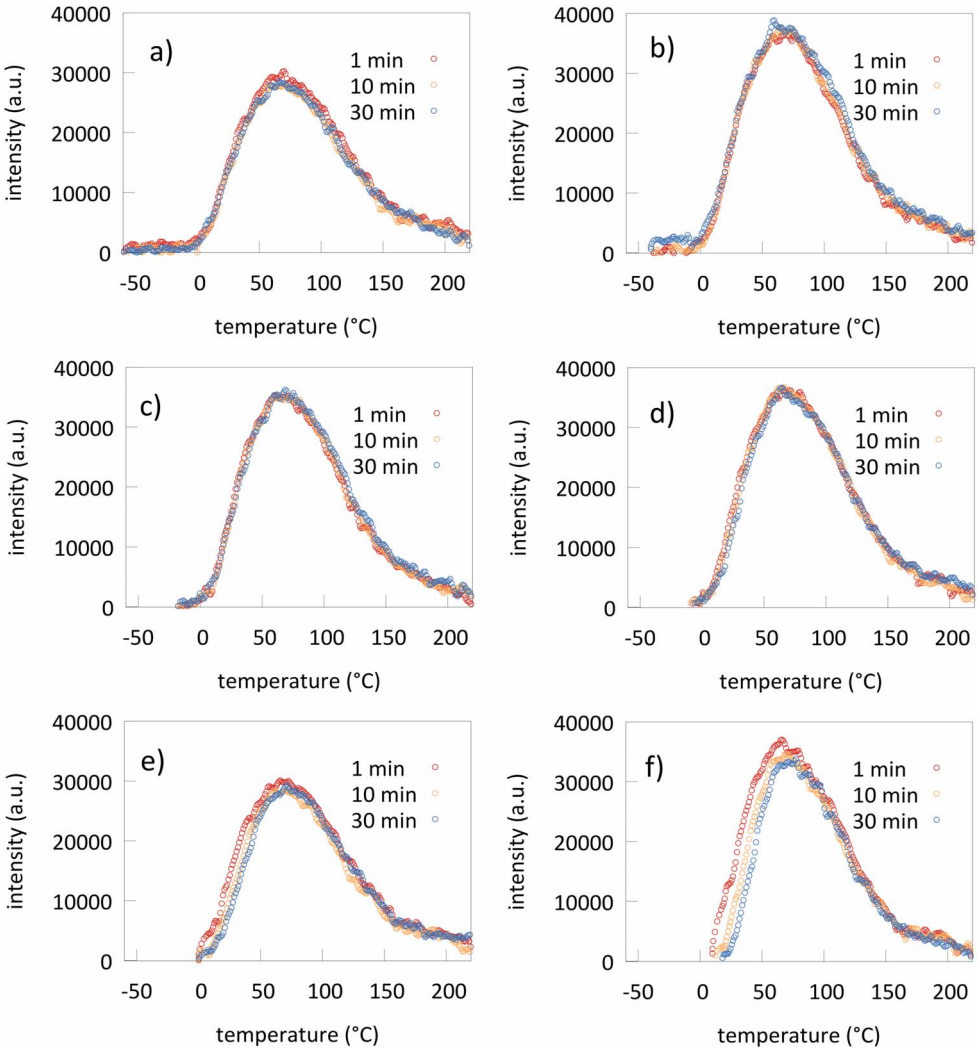


Figure 5. Thermal fading behavior for LGO:Cr, charged at 20°C with 254 nm excitation during 10 min and afterwards cooled to: a) −60°C, b) −40°C, c) −20°C, d) −10°C, e) 0°C and f) 10°C. The fading times for each measurement were 1, 10 and 30 min.

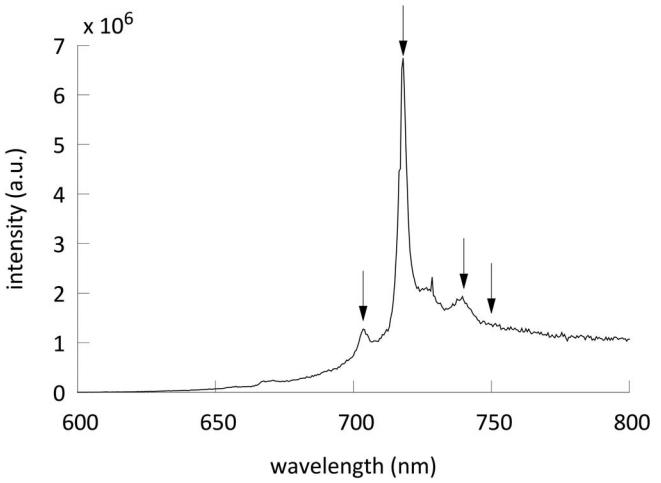


Figure 6. Steady-state PL spectrum of LGO:Cr, under excitation with 280 nm light. The points that are monitored over time in the afterglow are indicated by the arrows at 703.5 nm, 718 nm, 740 nm and 750 nm.

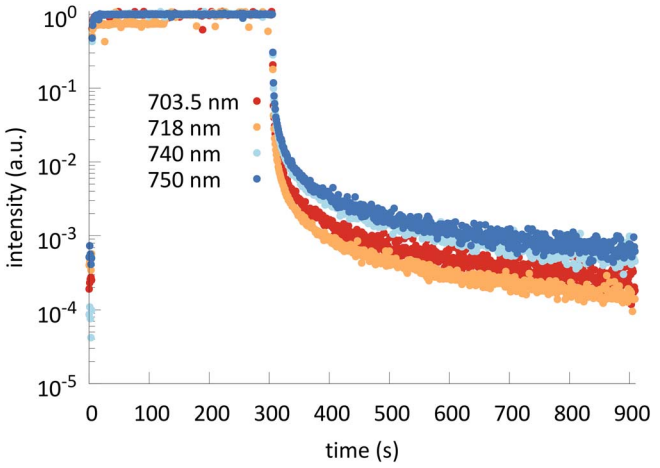


Figure 7. Time evolution of the spectrum of LGO:Cr. The intensities are normalized to the intensity during steady-state PL in the first 300 s. After excitation is stopped, the spectral afterglow is monitored for 10 min. There is a diverging, wavelength-dependent decay behavior, caused by a varying NBR.

temperatures (Figure 5f). This indicates that trap depletion is thermally controlled from −10°C onwards. Both Templer and McKeever and Chen[25,30] have argued that if a tunneling process occurs in the phosphor, it is more likely from the deeper-lying trap states. This would lead to a temperature-independent decrease of the TL signal, which would be more pronounced on the high temperature side of the TL peak. On the other hand, the temperature-dependent decrease of the TL peak at the low temperature side, which we measure here, is consistent with the localized transition model, first developed by Halperin and Braner,[31] which states that recombination occurs via a shared excited state between trap and recombination center.

Taking the above into consideration, the detrapping at RT is thus dominated by a thermally activated, local transition, even though a small and negligible contribution from tunneling cannot be excluded.

Additional insight in the thermally activated detrapping can be gained from monitoring the afterglow spectrum of Cr. As the Cr^{3+} luminescence is highly sensitive to the local surroundings in the host lattice and nearby defects,[19,32–35] changes in the spectrum over time can reveal a specific subset of Cr ions that take part in the afterglow.

Figure 6 shows the steady-state PL spectrum of LGO:Cr. The narrow emission line at 718 nm is the zero-phonon R-line, corresponding to a spin-forbidden transition from the ^2E state to the $^4A_2$ ground state.[36] The R-line is accompanied by Stokes- and anti-Stokes phonon sidebands at 703.5 nm, 727 nm and 740 nm. The separation between the zero-phonon line and the phonon side bands falls in range from 200–400 cm^{-1}, in agreement with literature values obtained from FTIR and Raman spectroscopy.[19,37]

The ^2E lines are situated on top of a broad emission band, from 650 nm to over 800 nm, that is due to a spin-allowed transition between the $^4T_2$ state and the ground state. Thus, at each wavelength, there will be a contribution to the total emission from both the ^2E and $^4T_2$ levels. The shape of the chromium PL spectrum can thus be described in terms of a Narrow-to-Broad-band emission Ratio (NBR), i.e. $NBR(\lambda) = I_{2_E}(\lambda) / I_{4_{T_2}}(\lambda)$. We will use the notational shorthand NBR in the following.

The steady-state PL spectrum is the average spectrum of all the chromium ions present in the material. Different Cr ions are subject to a local crystal field, which is influenced by e.g. the presence of defects in the first coordination shells of Cr. As such, variation of the spectrum with time reflects that particular chromium ions are taking part in the afterglow. Especially the evolution of the NBR reflects that chromium ions in different environments take part in the afterglow.

The decay of the emission was monitored at four distinct wavelengths (indicated by the arrows in Figure 6) for 10 min after stopping the excitation. The results are shown in Figure 7. If the NBR does not vary in time, the normalized decay profiles should perfectly overlap with one another. It is immediately clear that this is not the case. The 718 nm line decays much faster than, e.g., the emission at 750 nm, corresponding to $^4T_2$ emission.

As can be understood from the Tanabe-Sugano diagrams for $3d^3$ ions, the energy difference between the excited ^2E and $^4T_2$ levels varies according to the crystal field strength at the chromium site. If the energy difference is small enough, emission from both levels can occur. The lower the crystal field, the more emission from the $^4T_2$ level will contribute to the global emission profile. Dominating $^4T_2$ transitions in the spectrum of Cr^{3+} are thus indicative of chromium ions that are subject to smaller crystal fields in their nearest neighbor shell.[35,38–40]

Hence, the varying decay spectrum is another indication for the presence of a trap distribution in LGO. Small variations in the local defect structure cause a variation in the depth of the trap levels, and thus a variation in time constant for the detrapping. From the dominating $^4T_2$ character in the afterglow spectrum, we can deduce that the deeper-lying traps correspond to defects that cause a decrease in crystal field at Cr sites; possibly by lengthening of the Cr-O bonds. Vacancies of different kinds, that are formed during the synthesis of LGO, could be causing this.

Furthermore, the variation in the NBR indicates that the detrapping mechanism in LGO:Cr is a local one. If detrapping is global and trapped charge-carriers are transported via the valence or conduction bands, we expect the afterglow spectrum to also be an average spectrum of all chromium ions in different surroundings. As such, the afterglow should decay without any changes in the afterglow spectrum.

As shown in Figure 2, codoping with M^{4+} enhances the afterglow. Measured TL curves for codoped samples show that the glow curve shifts to higher temperatures, corresponding to an increase of the number of deeper-lying traps (Figure 3). M^{4+} ions are expected to incorporate on the Ga^{3+} sites in LGO spinel, creating positively-charged point defects in the process ($Si_{Ga}^{\bullet}$ or $Ge_{Ga}^{\bullet}$, in Kröger-Vink notation[41]). Furthermore, due to the need for charge compensation, codoping with M^{4+} will induce additional, negatively charged defects. Cation vacancies (V_{Li}',V_{Ga}''') seem the most probable candidates for these defects. The presence of such vacancies can be verified from CL measurements on LGO and similar gallates (not shown here), where blue broadband emission arises around 400 nm.[42,43] This characteristic CL emission has been linked to Li and Ga vacancies in the host.[43,44]

The hypothesized trapping mechanism for Cr-based persistent phosphors entails that the trapped charged carriers are both holes and electrons, that are simultaneously separated from the excited Cr^{3+}

ions during charging.[9,15,16] In LGO, a similar trapping mechanism is possible if, for example, electrons are trapped at nearby, positively-charged oxygen vacancies or M^{4+} sites, and holes at the negative cation vacancies. Modeling the energy levels of the defect by ab initio computational means (e.g. via DFT calculations) could elucidate the nature of the traps that take part in the trapping and detrapping processes at RT.

Conclusions

LGO:Cr is an efficient afterglow phosphor, showing persistent luminescence for several hours before the intensity decreases below 10^{-3} mW sr^{-1} m^{-2}. The afterglow can be strongly enhanced by the addition of Si and Ge in the host.

There are strong indications for the presence of a broad trap distribution in the LGO:Cr phosphor: the afterglow intensity follows a hyperbolic t^{-1} behavior, and the TL signal is comprised of a broad glow peak extending to a continuous signal at higher temperatures. Thermal fading experiments have shown that trap depletion is thermally activated and is consistent with a localized transition model, in contrast with a temperature-independent tunneling process as described previously.

The fact that the afterglow spectrum changes with time, confirms that the detrapping occurs locally and that different Cr ions experience different crystal fields. Furthermore, the variation of the ratio between the narrow-band and broad-band emission of Cr^{3+} with time is another indication of the presence of a trap distribution.

The change in shape of the chromium emission shows that deeper traps correspond to defects that will lower the crystal field in the chromium neighborhood. Cation vacancies are the most probable candidate for this. Codoping LGO:Cr with Si or Ge increases the number of deep traps in the phosphor, as shown with TL.

Acknowledgments

O.Q. De Clercq gratefully acknowledges the financial support of the Ghent University's Special Research Fund (BOF). The authors also thank P.F. Smet, J.J. Joos and D. Van der Heggen for their insights and fruitful discussions.

ORCID

Olivier Q. De Clercq https://orcid.org/0000-0002-1900-4664
Dirk Poelman https://orcid.org/0000-0002-3930-172X

References

1. Q. le Masne de Chermont, C. Chaneac, J. Seguin, F. Pelle, S. Maitrejean, J. P. Jolivet, D. Gourier, M. Bessodes, and D. Scherman, *Proceedings of the National Academy of Sciences of the United States of America*, **104**(22), 9266 (2007).
2. Y. Zhuang, Y. Katayama, J. Ueda, and S. Tanabe, *Optical Materials*, **36**(11), 1907 (2014).
3. B. Viana, S. K. Sharma, D. Gourier, T. Maldiney, E. Teston, D. Scherman, and C. Richard, *Journal of Luminescence*, **170**, 879 (2016).
4. S. K. Singh, *RSC Adv.*, **4**(102), 58674 (2014).
5. J. Frangioni, *Current Opinion in Chemical Biology*, **7**(5), 626 (2003).
6. A. Bessière, S. Jacquart, K. Priolkar, A. Lecointre, B. Viana, and D. Gourier, *Optics express*, **19**(11), 10131 (2011).
7. Z. Pan, Y. Y. Lu, and F. Liu, *Nature materials*, **11**(1), 58 (2011).
8. F. Liu, W. Yan, Y. J. Chuang, Z. Zhen, J. Xie, and Z. Pan, *Scientific reports*, **3**, 1554 (2013).
9. J. Xu, J. Ueda, Y. Zhuang, B. Viana, and S. Tanabe, *Applied Physics Express*, **8**(4), 042602 (2015).
10. E. Teston, S. Richard, T. Maldiney, N. Lievre, G. Y. Wang, L. Motte, C. Richard, and Y. Lalatonne, *Chemistry*, **21**(20), 7350 (2015).
11. X. Fu, C. Liu, J. Shi, H. Man, J. Xu, and H. Zhang, *Optical Materials*, **36**(11), 1792 (2014).
12. K. Van den Eeckhout, P. F. Smet, and D. Poelman, *Materials*, **3**(4), 2536 (2010).
13. P. F. Smet, K. Van den Eeckhout, O. Q. De Clercq, and D. Poelman, in *Handbook on the Physics and Chemistry of Rare Earths*, B. Jean-Claude and K. P. Vitalij, eds., Volume 48, p. 1–108, Elsevier, (2015).
14. K. Korthout, K. Van den Eeckhout, J. Botterman, S. Nikitenko, D. Poelman, and P. F. Smet, *Physical Review B*, **84**(8), (2011).
15. D. Gourier, A. Bessière, S. K. Sharma, L. Binet, B. Viana, N. Basavaraju, and K. R. Priolkar, *Journal of Physics and Chemistry of Solids*, **75**(7), 826 (2014).
16. A. Bessière, S. K. Sharma, N. Basavaraju, K. R. Priolkar, L. Binet, B. Viana, A. J. J. Bos, T. Maldiney, C. Richard, D. Scherman, and D. Gourier, *Chemistry of Materials*, **26**(3), 1365 (2014).
17. C. Tydtgat, K. W. Meert, D. Poelman, and P. F. Smet, *Opt. Mater. Express*, **6**(3), 844 (2016).
18. A. De Vos, K. Lejaeghere, D. E. P. Vanpoucke, J. J. Joos, P. F. Smet, and K. Hemelsoet, *Inorganic chemistry*, **55**(5), 2402 (2016).
19. O. Q. De Clercq, L. I. D. J. Martin, K. Korthout, J. Kusakovskij, H. Vrielinck, and D. Poelman, *Journal of Materials Chemistry C*, Advance article (2017).
20. R. Visocekas, N. A. Spooner, A. Zink, and P. Blanc, *Radiation Measurements*, **23**(2–3), 377 (1994).
21. P. Avouris and T. N. Morgan, *The Journal of Chemical Physics*, **74**(8), 4347 (1981).
22. M. Jain, B. Guralnik, and M. T. Andersen, *Journal of physics. Condensed matter: an Institute of Physics journal*, **24**(38), 385402 (2012).
23. J. T. Randall and M. H. F. Wilkins, *Proceedings of the Royal Society of London. Series A. Mathematical and Physical Sciences*, **184**(999), 365 (1945).
24. W. F. Hornyak and R. Chen, *Journal of Luminescence*, **44**(1), 73 (1989).
25. R. Templer, *Radiation Protection Dosimetry*, **17**(1-4), 493 (1986).
26. J. Botterman, J. J. Joos, and P. F. Smet, *Physical Review B*, **90**(8), (2014).
27. R. Chen and S. W. McKeever, *Theory of Thermoluminescence and Related Phenomena*, World Scientific, 1997.
28. K. Van den Eeckhout, A. J. J. Bos, D. Poelman, and P. F. Smet, *Physical Review B*, **87**(4), (2013).
29. Y. Katayama, B. Viana, D. Gourier, J. Xu, and S. Tanabe, *Opt. Mater. Express*, **6**(4), 1405 (2016).
30. S. McKeever and R. Chen, *Radiation Measurements*, **27**(5), 625 (1997).
31. A. Halperin, A. Braner, A. Ben-Zvi, and N. Kristianpoller, *Physical Review*, **117**(2), 416 (1960).
32. W. Mikenda, *Journal of Luminescence*, **26**, 53 (1981).
33. W. Mikenda, *Journal of Luminescence*, **26**, 67 (1981).
34. W. Mikenda, *Journal of Luminescence*, **26**, 85 (1981).
35. G. Imbusch and B. Henderson, Clarendon Press, Oxford, 1989.
36. H. Szymczak, M. Warddzynska, and I. E. Mylnikova, *Journal of Physics C: Solid State Physics*, **8**, 3937 (1975).
37. V. G. Keramidas, B. A. Deangelis, and W. B. White, *Journal of Solid State Chemistry*, **15**(3), 233 (1975).
38. Y. Tanabe and S. Sugano, *Journal of the Physical Society of Japan*, **9**(5), 753 (1954).
39. Y. Tanabe and S. Sugano, *Journal of the Physical Society of Japan*, **9**(5), 766 (1954).
40. Y. Tanabe and S. Sugano, *Journal of the Physical Society of Japan*, **11**(8), 864 (1956).
41. F. A. Kröger and H. J. Vink, *Solid State Physics*, **3**, 307 (1956).
42. G. Blasse and A. Bril, *Materials Research Bulletin*, **5**(4), 231 (1970).
43. K.-S. Suh, S.-J. Jang, K.-I. Cho, S. Nahm, and J.-D. Byun, *Journal of Vacuum Science & Technology B: Microelectronics and Nanometer Structures Processing, Measurement, and Phenomena*, **16**(2), 858 (1998).
44. L. Binet and D. Gourier, *Journal of Physics and Chemistry of Solids*, **59**(8), 1241 (1998).